© 2016. Published by The Company of Biologists Ltd | Development (2016) 143, 4381-4393 doi:10.1242/dev.139840

STEM CELLS AND REGENERATION

RESEARCH ARTICLE

Distinct capacity for differentiation to inner ear cell types by progenitor cells of the cochlea and vestibular organs

Will J. McLean[1,2,3], Dalton T. McLean[1,2], Ruth Anne Eatock[4,*] and Albert S. B. Edge[1,2,3,5,*]

ABSTRACT

Disorders of hearing and balance are most commonly associated with damage to cochlear and vestibular hair cells or neurons. Although these cells are not capable of spontaneous regeneration, progenitor cells in the hearing and balance organs of the neonatal mammalian inner ear have the capacity to generate new hair cells after damage. To investigate whether these cells are restricted in their differentiation capacity, we assessed the phenotypes of differentiated progenitor cells isolated from three compartments of the mouse inner ear – the vestibular and cochlear sensory epithelia and the spiral ganglion – by measuring electrophysiological properties and gene expression. Lgr5$^+$ progenitor cells from the sensory epithelia gave rise to hair cell-like cells, but not neurons or glial cells. Newly created hair cell-like cells had hair bundle proteins, synaptic proteins and membrane proteins characteristic of the compartment of origin. PLP1$^+$ glial cells from the spiral ganglion were identified as neural progenitors, which gave rise to neurons, astrocytes and oligodendrocytes, but not hair cells. Thus, distinct progenitor populations from the neonatal inner ear differentiate to cell types associated with their organ of origin.

KEY WORDS: Hair cell, Neuron, Neural stem cell, Cochlea, Vestibular, Spiral ganglion, Mouse

INTRODUCTION

Impaired hearing (15% of the population) and balance (35%) associated with a risk of falling and severely reduced quality of life (Agrawal et al., 2009) most commonly reflect sensory hair cell (HC) loss (Wong and Ryan, 2015) or auditory synapse degeneration (Kujawa and Liberman, 2009; Spoendlin, 1975). The permanence of hearing loss is likely to be related to the lack of regenerative capacity in the adult cochlea, where HC damage is not followed by differentiation of new cells. However, recent demonstrations of spontaneous HC regeneration in neonatal cochlea suggest the continued presence of progenitor cells (Bramhall et al., 2014; Cox et al., 2014). Replacement of HCs in the neonate is achieved primarily by transdifferentiation of supporting cells and not by proliferation of progenitor cells. A low level of regeneration of vestibular HCs has also been observed but decreases with age (Burns et al., 2012) and is not sufficient to compensate for loss of HCs (Burns et al., 2012; Rauch et al., 2001).

Neural progenitors that give rise to different brain regions during development are initially broadly specified and then become increasingly restricted to specific fates corresponding to location, as has been shown by the maintenance of regional phenotypes by cells cultured as neurospheres (Hitoshi et al., 2002). In a similar process, early embryonic progenitors in the otic placode are specified to make the hearing and balance organs of the inner ear – the cochlea and vestibular organs – with specialized neurons, sensory HCs and supporting cells. This occurs through a well-choreographed series of steps involving both innate genetic programs and inductive cues (Barald and Kelley, 2004; Groves et al., 2013; Raft and Groves, 2015). In previous studies, cells isolated from cochlear, vestibular, and neural inner ear compartments in the early postnatal mouse formed spheres that were thought to be multipotent, i.e. capable of generating neurons, HCs and glia (Li et al., 2003; Malgrange et al., 2002; Martinez-Monedero et al., 2008; Oshima et al., 2007), or were even reported to be pluripotent, i.e. capable of forming all cell types in the organism (Li et al., 2003). The putative HCs expressed electrophysiological properties of embryonic HCs (Oshima et al., 2007) and the putative neurons were glutamatergic and had properties of cochlear afferent neurons (Martinez-Monedero et al., 2008). The cells within the spheres, however, whether generated from cochlear, vestibular, or spiral ganglion compartments of the inner ear, were heterogeneous, and it was not possible to determine whether single progenitor cells gave rise to multiple differentiated types or whether several progenitor populations existed within a given inner ear compartment.

Evidence from the intact cochlear epithelium (organ of Corti, OC) suggests that postnatal supporting cells are not uniform. A subset of supporting cells in the early postnatal mouse OC expresses Lgr5 (Chai et al., 2012; Shi et al., 2012), a marker of stem cells of the intestinal epithelium (Barker et al., 2007). Lgr5 increases a cell's responsiveness to Wnt by potentiating the signal transmitted through frizzled (de Lau et al., 2011). Forced activation of the Wnt pathway in Lgr5$^+$ cells in the neonatal OC caused proliferation of Lgr5$^+$ supporting cells as well as their differentiation to HCs (Shi et al., 2013). HC regeneration in the neonate also occurred from Lgr5$^+$ cells and required Wnt pathway activation, whether spontaneous or induced by Notch inhibition (Bramhall et al., 2014). We used Lgr5 as a marker for the HC progenitors in the cochlea and vestibular systems in these experiments to determine the cell types produced from spheres during differentiation.

We also investigated whether specific inner ear cell types could be generated from any compartment or only from the compartment of origin, i.e. spiral ganglion, vestibular epithelium or OC. Potency of neural stem cells has been difficult to determine without adequate markers to use for tracing the lineage of progenitor cells and for the differentiated progeny, and, as a result, similar questions have

[1]Department of Otology and Laryngology, Harvard Medical School, Boston, MA 02114, USA. [2]Eaton-Peabody Laboratories of Auditory Physiology, Massachusetts Eye and Ear Infirmary, Boston, MA 02114, USA. [3]Program in Speech and Hearing Bioscience and Technology, Division of Health Sciences and Technology, Harvard & MIT, Cambridge, MA 02139, USA. [4]Department of Neurobiology, University of Chicago, Chicago, IL 60637, USA. [5]Harvard Stem Cell Institute, Cambridge, MA 02138, USA.

*Authors for correspondence (eatock@uchicago.edu; albert_edge@meei.harvard.edu)

A.S.B.E., 0000-0001-8641-755X

Received 3 June 2016; Accepted 11 October 2016

Development (2016) 143, 4381-4393 doi:10.1242/dev.139840

remained unresolved in several neural and non-neural stem cell compartments (Fuentealba et al., 2015). Here, by using gene expression analysis and physiological properties, as well as lineage tracing of putative progenitors in the spiral ganglion, OC and vestibular epithelia, we could identify nine distinct cell types, which allowed us to determine whether the progenitor cells were uni-, multi- or pluripotent. Our results indicate that postnatal inner ear progenitors are restricted to the lineages of their respective organs of origin, although newly identified PLP1^{+} progenitor cells within the auditory nerve also form glial cell types of the central nervous system.

RESULTS

Progenitor cells from three compartments in the inner ear

We performed experiments on the differentiation of progenitors from three compartments of the inner ear (Fig. 1) from the early postnatal mouse: the OC, the vestibular epithelia (the utricular macula, saccular maccula and semicircular canal cristae combined) and the spiral ganglion (containing Schwann cells and cell bodies of cochlear neurons). We cultured cells in conditions that produced spheres by cell division (Materials and Methods). We then differentiated the spheres for 14-70 days to allow significant maturation and used distinct markers and electrophysiological features to achieve cell-specific identification as shown in Figs 2–4. We used lineage tracing with Lgr5 and PLP1, respectively, to follow cell fates of epithelial and spiral ganglion progenitors (described in Figs 5–7). The combination of progenitor-specific lineage tags and cell-specific markers allowed us to identify the cell types produced by progenitor cells in each compartment of these closely related cell types, which had not been possible in previous experiments (Li et al., 2003; Oshima et al., 2007).

HC proteins in cells differentiated from inner ear progenitors

To ensure that results were not significantly affected by HCs carried over from the original dissociated tissue, we counted the number of HCs that were still present after the third passage. HCs were recognized by their expression of the HC markers Atoh1-nGFP (visualized by GFP fluorescence) and myosin VIIA (visualized by immunostaining). Third-generation spheres were seeded in the same experimental culturing conditions as were used for differentiation analysis experiments, but instead were only allowed to differentiate for 3 h. This seeding time allowed the spheres to adhere to the culturing surface, but was too short for the cells to differentiate. The cells were viewed by confocal microscopy over the entire seeding area. Cochlear spheres that were differentiated for 3 h gave rise to no Atoh1-nGFP-expressing cells; 14 days of differentiation produced an average of 32±12 Atoh1-nGFP^{+} cells (n=3 cultures). For vestibular spheres, 3 h of differentiation produced one Atoh1-nGFP^{+} cell (n=2 cultures), substantially fewer than the average after 14 days (326±107 Atoh1-nGFP^{+} cells; n=4 cultures). We also did RT-PCR analysis on third-generation spheres collected from floating cultures (n=3 cultures) to look for expression of the hair-cell marker myosin VIIA. These spheres were positive for GAPDH but negative for the hair-cell marker myosin VIIA, unlike spheres that were differentiated longer. In all, these results indicate that our results on differentiated inner ear spheres reflect production of new HC-like cells and are not caused by native cells that survived the culturing process, consistent with previous work using this method (Martinez-Monedero et al., 2008).

Differentiated spheres contained cells that stained for HC markers, such as the transcription factor Atoh1 (Bermingham et al., 1999), detected in an Atoh1-nGFP mouse (Lumpkin et al., 2003), myosin VIIA (Grati and Kachar, 2011; Hasson et al., 1995) and the Ca^{2+}-binding protein parvalbumin (Yang et al., 2004). We refer to these cells as 'hair cell-like cells'. Atoh1-nGFP^{+} cells were a small fraction (~1%; 876/92443) of all cells in the differentiated spheres. Fifty-one percent of Atoh1-nGFP^{+} cells double-stained for another HC marker, such as myosin VIIA, which is similar to the 44% yield of <1% of total cells in culture found in a previous study (Oshima et al., 2007). Sixty-seven percent (285/423) of myosin VIIA-positive cells derived from vestibular progenitors and 81% (690/850) of myosin VIIA-positive cells derived from cochlear progenitors had protruding structures that were labeled by phalloidin (Fig. 2A-C,F,H), which stains filamentous actin, the most abundant protein in stereocilia. Of phalloidin-positive structures, 50% (27/54) from cochlear progenitors and 73% (58/79) from vestibular progenitors were immunoreactive for plasma membrane Ca^{2+}-ATPase 2 (PMCA2; also known as Atp2b2; Fig. 2C,H), which is abundant in postnatal HC bundles (Chen et al., 2012; Dumont et al., 2001; Hill et al., 2006). PMCA2-like immunoreactivity was strong at the base of the actin-positive structures (Fig. 2C,H, arrows), as reported for HCs (Chen et al., 2012), with more diffuse immunoreactivity present in the membrane of the cell body (Fig. 2C,H, arrowheads). Some of the phalloidin-positive structures resemble actin-containing 'cytocauds', a malformation of stereocilia that has been described in animals with inner ear mutations affecting hair bundles (Kanzaki et al., 2002).

In addition to the actin-based stereocilia, vestibular hair bundles and immature cochlear hair bundles have a single kinocilium that is microtubule based and contains acetylated α-tubulin (Li et al., 2008; Ogata and Slepecky, 1995). In our differentiated cells, immunoreactivity to acetylated α3 tubulin was rare: only 4% (9/289) of vestibular hair cell-like cells (Fig. 2B; Table 1) and no cochlear hair-cell like cells (0/312) were stained. Phalloidin-positive rings near Atoh1-nGFP^{+} cells (Fig. 2I, asterisk) are reminiscent of actin rings that typically surround supporting cells in HC epithelia (Burns and Corwin, 2014), suggesting that spheres form partially organized epithelia during differentiation.

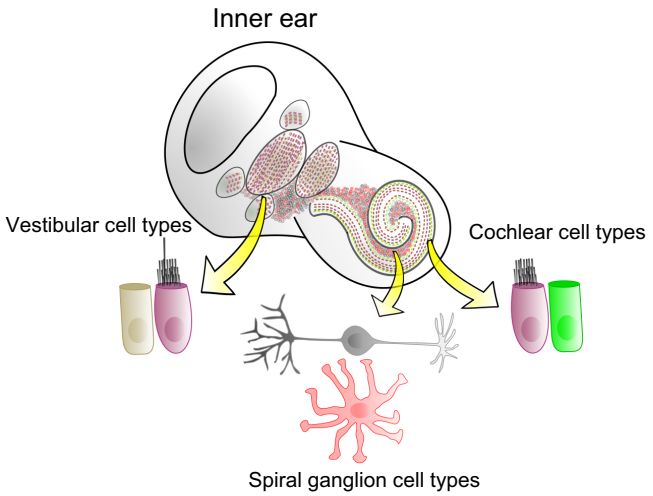

Fig. 1. Overview of cell types in three compartments of the inner ear. (1) Vestibular epithelia, containing sensory hair cells (purple) and supporting cells (beige); (2) the cochlear OC, comprising sensory HCs (purple) and Lgr5^{+} supporting cells (green); and (3) the spiral ganglion comprising Schwann cells (red) and primary afferent neurons (gray). HC-like cells produced from vestibular and cochlear compartments were analyzed, and the potencies of Lgr5^{+} cells within the OC and PLP1^{+} glial cells within the spiral ganglion examined.

Development (2016) 143, 4381-4393 doi:10.1242/dev.139840

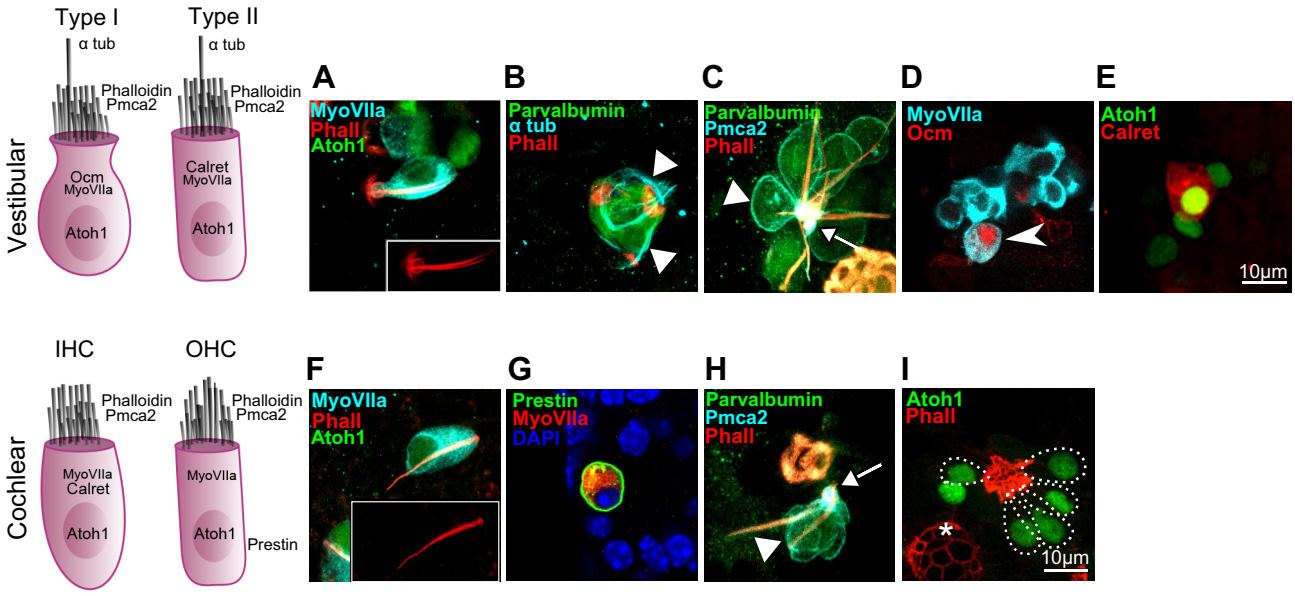

Fig. 2. Progenitor cells derived from vestibular organs and OC can differentiate into cells that express HC proteins and other typical HC characteristics. On the left are cartoons of the major HC types and some of their key proteins found in vestibular (top) and cochlear (bottom) intact, mature inner ear epithelia. (A-E) Vestibular-derived cells identified as HC-like by Atoh1 expression had other HC-like features, including strong intracellular labeling for myosin VIIa (A,D) and the Ca^{2+}-binding proteins parvalbumin (B), oncomodulin (Ocm; D, arrowhead) which is specific to type I vestibular HCs *in vivo*, and calretinin (Calret; E); phalloidin-positive apical structures that are reminiscent of cuticular plates and stereocilia (A-C) and, like stereocilia, stain for PMCA2 (C; arrowhead points to staining of the membrane, and arrow points to white structure where three labels colocalize); and elongated structures that, like the kinocilia of vestibular hair bundles, are immunoreactive for α3 acetylated tubulin (B, multiple cells with multiple tubulin-positive structures, e.g. arrowheads). (F-I) Cochlear-derived HC-like cells, recognized by expression of Atoh1 (F,I), myosin VIIA (F,G) or parvalbumin (H), had phalloidin-stained (F,I) or PMCA2-immunoreactive (H; arrowhead shows diffuse staining in the membrane and arrow points to colocalization of all three labels) bundle-like structures emanating from the apical surface. Many showed strong immunoreactivity in the lateral membrane to prestin (G), the electromotility motor specific to OHCs. (I) Actin rings were also seen in cochlear-derived spheres. Here, they are at the apices of a cluster of $Atoh1^+$ HC-like cells (green; outlined), and also form an epithelial-like web of actin around other cells (asterisk), consistent with non-sensory epithelium. Phalloidin stain alone shown in insets in A and F. Scale bars in E,I apply to all micrographs.

To investigate whether any differentiated HC-like cells assume a specialized fate, we labeled them with antibody against prestin (Slc26a5), a membrane protein that is specifically expressed in cochlear outer HCs (OHCs) and not in vestibular organs (Zheng et al., 2000). In the OC, expression increases between postnatal day (P) 0 and the onset of hearing (~P12 in mice) (Belyantseva et al., 2000). OC-derived Atoh1-nGFP$^+$ cells showed robust prestin-like immunoreactivity in the cell membrane, always in conjunction with myosin VIIA immunoreactivity (Fig. 2G). The percentage of cells that were prestin positive (61%) is roughly consistent with the percentage of OHCs in the cochlea (~75%). By contrast, none of 1302 Atoh1-nGFP$^+$ cells generated from vestibular organs expressed prestin (Table 1). These data suggest that each inner-ear stem cell population is strongly biased to differentiate into a specific HC type, i.e. that the potency of each tissue is limited to cells specific to that tissue.

Table 1. Incidence of label for HC proteins

	Cochlear derived	Vestibular derived
Staining target	Cell count	Cell count
Phalloidin (actin; hair bundles)	690/850 MyoVIIa$^+$ cells (81%)	285/423 MyoVIIa$^+$ cells (67%)
α3 tubulin (kinocilia)	0/312 MyoVIIa$^+$ cells (0%)	9/289 MyoVIIa$^+$ cells (4%)
PMCA2 (bundles)	27/54 actin bundles (50%)	58/79 actin bundles (73%)
Oncomodulin (type I vestibular HC)	N/A	8/83 MyoVIIa$^+$ cells (10%)
Calretinin (type II vestibular HC, IHC)	0/26 Atoh1$^+$ cells (0%)	5/15 Atoh1$^+$ cells (33%)
Prestin (OHC)	58/95 Atoh1$^+$ cells (61%)	0/1302 Atoh1$^+$ cells (0%)

N/A, not applicable.

To test whether the vestibular spheres had a similar capacity for generating specific cell types, we stained for oncomodulin, a marker of type I HCs in the central zones of vestibular epithelia (Simmons et al., 2010) (Fig. 2D). Ten percent (8/83) of myosin VIIA-positive cells derived from vestibular progenitors showed oncomodulin-like immunoreactivity, the same as the percentage of HCs in the mature mouse utricular epithelium that are striolar type I HCs (366/3613; Li et al., 2008). The Ca^{2+}-binding protein calretinin (calbindin 2) is strongly expressed in immature HCs as well as in mature type II vestibular HCs and cochlear inner HCs (IHCs) (Dechesne et al., 1994; Desai et al., 2005; Li et al., 2008). The calretinin antibody labeled one-third of Atoh1-nGFP$^+$ cells (5/15 cells, one experiment) derived from vestibular tissue (Fig. 2E; Table 1). By contrast, no cochlear Atoh1-nGFP$^+$ cells (0/26) were calretinin positive; thus, if any cells were differentiating along the IHC path, they did not acquire all IHC properties.

In summary, immunostaining for the HC markers Atoh1 and myosin VIIA showed that some differentiating cells in spheres acquired proteins expected of HCs. Of these cells, many had protrusions containing F-actin and PMCA2, typical of stereocilia, but very few expressed the kinocilium marker α3 tubulin. The expression of prestin by a large fraction of HC-like cells derived from the OC but not by any cells derived from vestibular tissue suggests that the inner ear progenitor cells of the neonatal mouse are not fully competent to form HCs of all types, but rather have fates restricted to their inner ear compartment of origin. This might indicate differentiation limitations in each organ's progenitor cell population.

Development (2016) 143, 4381-4393 doi:10.1242/dev.139840

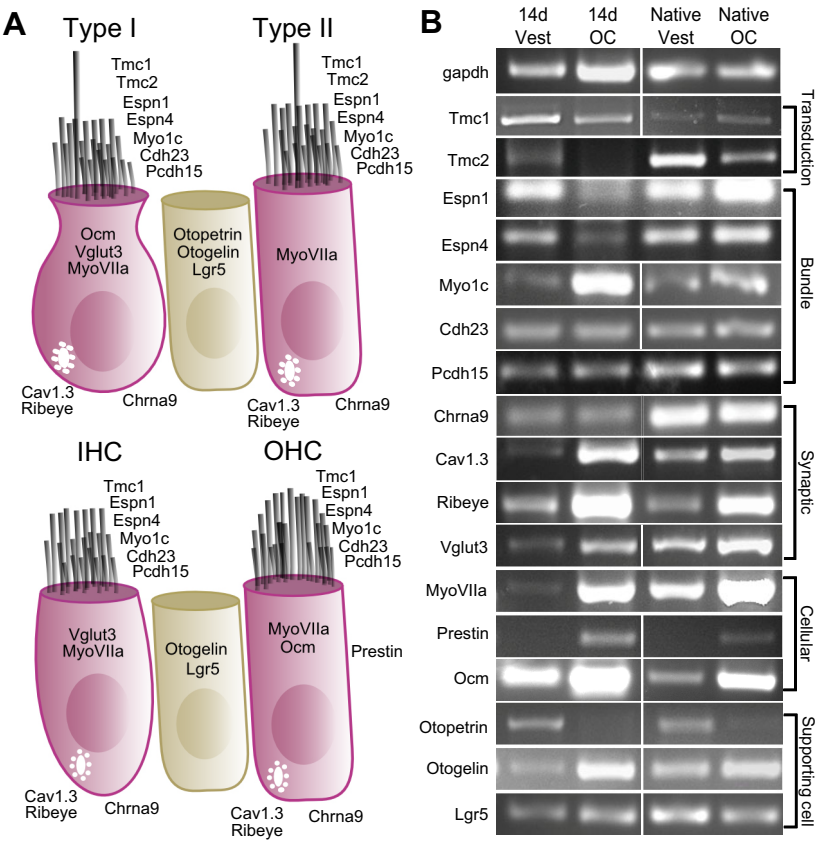

Fig. 3. Differentiated OC and vestibular cultures expressed genes that are specific to their tissue of origin and are required for proper physiological function. (A) Schematic showing the genes that were analyzed and their approximate *in vivo* localization within each tissue, cell type and cellular compartment (hair bundle, cytoplasm of the cell body, or synapse). (B) Differentiated cells from both tissues expressed the HC gene myosin VIIA, hair-bundle associated genes (*Espn1*, *Espn4*, *Myo1c*, *Cdh23*, *Pchd15*), genes associated with synaptic function (*Chrna9*, *Vglut3* and genes for $Ca_V1.3$ and Ribeye) and Ca^{2+} binding (*Ocm*), and the supporting cell genes otogelin and *Lgr5*. Cells of vestibular and cochlear origin differed in prestin, otopetrin and Tmc2 expression. All results were confirmed with five or more sphere cultures. Native cochlear and vestibular data were from tissues at P5. *Gapdh* was used as a positive control. Marker lanes and lanes for water (negative control) are not shown. (n=5 per gene).

Expression of hair cell-specific genes

We next used RT-PCR to detect mRNA that is essential for proper HC functions and would further specify HC type. We probed differentiated spheres of OC and vestibular origin for mRNA specific to: the mechanosensory apparatus (Tmc proteins), hair bundles (espins), electromotility in OHCs (prestin), the presynaptic apparatus (proteins of synaptic ribbons and vesicles) and the postsynaptic apparatus (receptors for cholinergic efferent input) (Fig. 3A). We also tested for expression of genes related to supporting cell function, in particular secretion of the extracellular matrices (otogelin and otopetrin). The spheres were differentiated for 14 days and expression is compared with control data from native tissues prepared acutely at P5. Representative gels for these probes are shown in Fig. 3B and the results are summarized here.

In HCs, Tmc proteins are essential for mechanoelectrical transduction (Pan et al., 2013). In both vestibular and cochlear native tissues at P5, we detected expression of mRNA for both isoforms Tmc1 and Tmc2, as expected. Vestibular-derived differentiated cells expressed Tmc1 and Tmc2, and OC-derived cells expressed Tmc1. The lack of Tmc2 in OC-derived cells might indicate differentiation of the transduction complex, consistent with the *in vivo* time course: Tmc2 disappears from the OC at about the onset of hearing (Pan et al., 2013), and the spheres were differentiated for 14 days at a minimum.

Differentiated progenitors and native tissues all expressed myosin 1c, which plays a key role in transducer adaptation in vestibular HCs (Gillespie, 2004; Holt et al., 2002), and the tip-link proteins, cadherin 23 and protocadherin 15, which are crucial for transduction (Kazmierczak et al., 2007). Differentiated progenitor cells from both vestibular and OC tissues expressed two isoforms of espin, espin1 and espin4, which are associated with stereociliary elongation. Given that espin4 arises postnatally (Sekerková et al., 2006), its presence further suggests that some hair cell-like cells had differentiated significantly.

We also found that differentiated progenitors from both tissues expressed genes that are specific to afferent and efferent synaptic functions. At afferent synapses from HCs onto neurons, Ca^{2+} enters through $Ca_V1.3$ (Cacna1d) calcium channels (Dou et al., 2004; Platzer et al., 2000) in the pre-synaptic HC membrane to promote release of glutamate from vesicles clustered around presynaptic ribbons. As shown in Fig. 3B, differentiated spheres from both tissues expressed the genes encoding the vesicular glutamate transporter Vglut3 (Slc17a8), which packages glutamate into hair-cell synaptic vesicles (Peng et al., 2013; Seal et al., 2008; Wang et al., 2007); C-terminal binding protein 2 (Ctbp2; also known as Ribeye), which is the major component of pre-synaptic ribbons (Schmitz et al., 2000); and $Ca_V1.3$ channels. HCs are innervated by efferent nerve fibers of brainstem origin, which release acetylcholine onto hair cell-specific cholinergic receptors containing α9 subunits encoded by *Chrna9* (Elgoyhen and Franchini, 2011; Luo et al., 1998). Differentiated spheres from both tissues expressed *Chrna9* (Fig. 3B). Expression of molecules specialized for inner ear synaptic transmission indicates that HC differentiation took place.

Consistent with our antibody staining, and confirming previous RT-PCR results on differentiated spheres (Oshima et al., 2007), the cells from both cochlea and vestibular organs expressed the hair-cell marker myosin VIIA, whereas cochlear spheres alone expressed the OHC marker prestin (Fig. 3B). Expression of the calcium-binding protein oncomodulin (Ocm) was detected in both cochlear and vestibular tissues, as expected from *in vivo* reports, where it is selectively expressed by vestibular type I cells and cochlear IHCs (Fig. 3B).

Development (2016) 143, 4381-4393 doi:10.1242/dev.139840

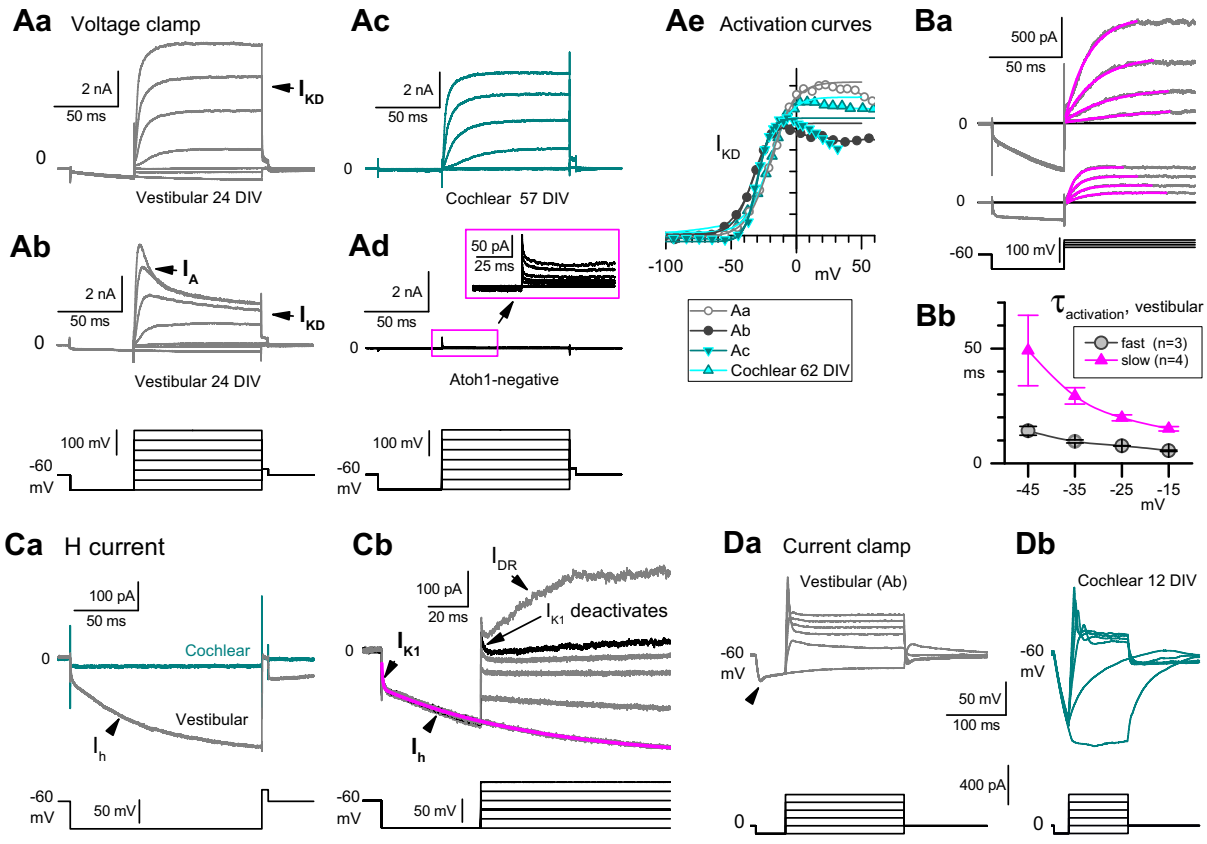

Fig. 4. Differentiated OC and vestibular progenitor cells resemble the HCs from their tissues of origin in certain electrophysiological properties. (A) Whole-cell currents evoked by voltage steps (shown below) in Atoh1-nGFP$^+$ cells derived from vestibular tissue (Aa, Ab; 24 days *in vitro*, DIV) and OC (Ac; 57 DIV), and in an Atoh1-nGFP-negative cell (Ad). In Atoh1-nGFP$^+$ cells, depolarizing voltage steps evoked large outward currents reminiscent of the delayed rectifier potassium currents (I_{DR}) found in native HCs (*n*=29 vestibular, *n*=32 cochlear). Some (Ab) but not all (see Aa) Atoh1-nGFP$^+$ cells from vestibular tissue had inactivating currents (I_A; *n*=4). Currents in Atoh1-nGFP-negative cells (Ad) were small (boxed area of trace enlarged in inset) and did not resemble those of native HCs (*n*=1 vestibular, *n*=6 cochlear). (Ae) Tail current activation curves taken at −40 mV, for the cells in Aa-Ac and another cochlear-derived Atoh1-nGFP$^+$ cell (62 DIV). Smooth curves are single-Boltzmann fits. (B) Outward currents from vestibular-derived Atoh1-nGFP$^+$ cells (Ba) had activation time courses that separated into two groups (Bb) with time courses of native type I HCs (slow) and type II HCs (fast) (*n*=3 slow, *n*=4 fast). (C) I_h was found in 65% of vestibular-derived Atoh1-nGFP$^+$ cells and no cochlear-derived Atoh1-nGFP$^+$ cells (Ca). Vestibular HCs also appeared to express the fast inward rectifier I_{K1} (Cb). In Cb, arrowheads point to fast activation of I_{K1} and slower activation of I_h at −125 mV; arrow points to fast deactivation of I_{K1} after step from −125 mV to −45 mV (*n*=19 I_{K1}, *n*=22 I_h). (D) Vestibular-derived (Da) and cochlear-derived (Db) Atoh1-nGFP$^+$ cells responded to current steps with heterogeneous voltage changes that are within the range of results from postnatal HCs (*n*=6 vestibular, *n*=4 cochlear).

Expression of supporting cell genes

Both otogelin (El-Amraoui et al., 2001) and Lgr5 are expressed by supporting cells in both the OC and vestibular epithelia, and otopetrin is specific to peripheral supporting cells of vestibular epithelia (Kim et al., 2010). Again, the differentiated spheres showed expression appropriate to their origins: spheres derived from both cochlear and vestibular tissue expressed otogelin and *Lgr5* mRNA, and only vestibular-derived spheres expressed otopetrin (Fig. 3B). Thus, sphere differentiation yields markers of inner-ear supporting cells in addition to HC markers.

In summary, both cochlear and vestibular progenitor cells can differentiate into cells that express components of the transduction apparatus, the hair bundle, and pre- and post-synaptic machinery, consistent with substantially differentiated HCs. The selective expression of prestin by OC-derived spheres and of Tmc2 and otopetrin by vestibular-derived spheres suggests that the progenitors from each tissue are constrained to differentiate into their native cell types.

Voltage-gated currents in differentiated hair cell-like cells

We conducted electrophysiological experiments on newly differentiated hair cell-like cells to test further the hypothesis that they form distinct cellular subtypes that are limited to those of their native organ, and to determine if their electrical properties resemble those reported for native HCs. With the patch clamp method, we recorded voltage-dependent whole-cell currents from HC-like cells, which we recognized in the recording dish by their expression of Atoh1-nGFP. Most Atoh1$^+$ cells produced large outwardly rectifying currents in response to depolarization, with amplitudes and time courses that are qualitatively within the range of the outward delayed rectifying K^+ current (I_{KD}) of HCs (Fig. 4A). We observed such currents in all (34/34) Atoh1$^+$ cells derived from vestibular organs (Fig. 4Aa,Ab) and in almost all (29/32; 91%) Atoh$^+$ cells derived from the cochlea (e.g. Fig. 4Ac). In the seven Atoh1-negative cells tested (six cochlear, one vestibular), none had HC-like currents (e.g. Fig. 4Ad).

To quantify the voltage dependence of steady-state outwardly rectifying currents, we made and fit tail-current activation curves

Development (2016) 143, 4381-4393 doi:10.1242/dev.139840

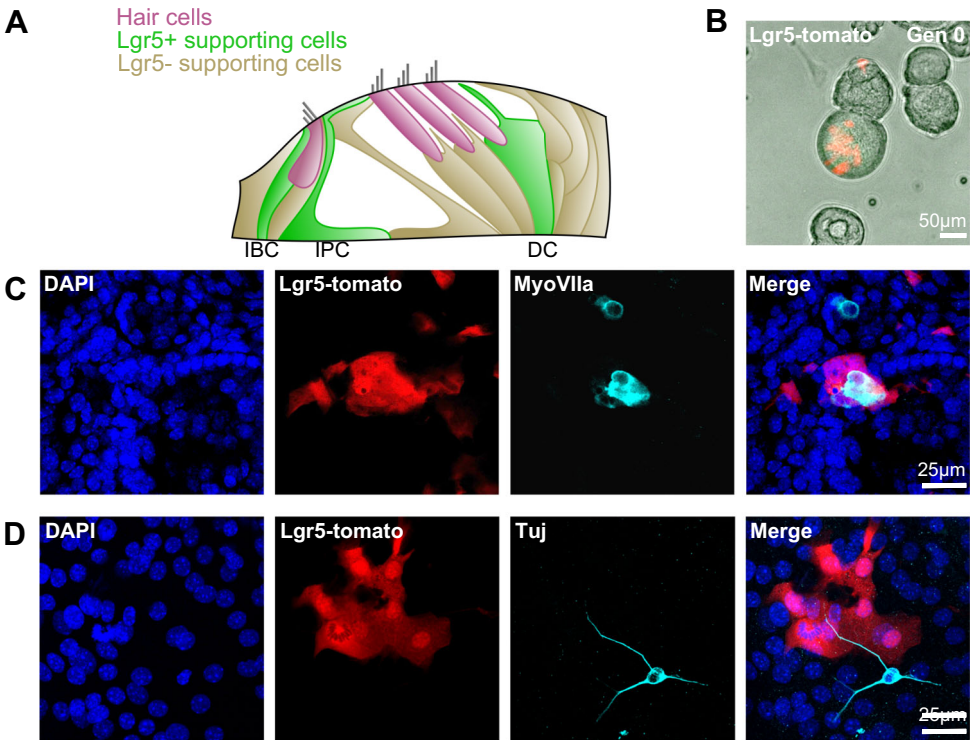

Fig. 5. Lgr5$^+$ cells from the postnatal cochlea form HCs but not neurons. (A) Schematic cross-section of the OC. Lgr5 is expressed in inner border cells (IBC), inner pillar cells (IPC), and Deiters' cells (DC). (B) Lgr5-tomato cells were present in cultured spheres after three passages and before differentiation. (C) Lineage-traced Lgr5-tdTomato cells gave rise to HC-like cells that were immunoreactive for myosin VIIA (n=20 MyoVIIa$^+$ cells). (D) Lgr5$^+$ cells did not form neurons in sphere culture (n=696 Tuj$^+$ cells). Here, antibody to Tuj1 stains a neuron-like cell with processes, and other cells are Lgr5-tdTomato-positive.

(Fig. 4Ae) from records like those in Fig. 4A (Materials and Methods). For both tissues of origin, I_{KD} activated around −60 mV and had activation midpoints ($V_{1/2}$ values) typical of mouse HCs of the first postnatal week (Marcotti et al., 2003a; Rüsch et al., 1998; reviewed by Eatock and Hurley, 2003), with means of −21±3 mV (±s.e.m.) and −33±2 mV for three cochlear and five vestibular cells, respectively. Negatively activating K^+ currents (I_{Kn} and $I_{K,L}$), which normally emerge in specific hair cells during the pre-hearing period in mice (Géléoc et al., 2004; Marcotti et al., 1999; Rüsch et al., 1998), were not detected here.

Outward currents in cochlear cells had activation time courses in the range recorded from neonatal cochlear HCs in *ex vivo* OC preparations (times to half-maximum current 10-20 ms) (Marcotti et al., 1999, 2003a). The activation time courses of outward currents of seven vestibular-derived cells (Fig. 4Ba) fell into two groups (Fig. 4Bb) with values close to those of type I and type II hair cells in the postnatal mouse utricle (Rüsch et al., 1998), consistent with differentiation of the vestibular progenitor cells into vestibular hair cell types. The outward currents of vestibular-derived cells showed a range of inactivation time courses, also consistent with reports from early postnatal mouse utricles (Holt et al., 1999; Rüsch et al., 1998): four out of 32 cells had strongly inactivating currents (A currents, I_A; Fig. 4Ab) whereas others did not show fast inactivation (Fig. 4Aa).

Vestibular-derived Atoh1$^+$ cells also resembled native vestibular HCs in expressing sizeable h currents, I_h, carried by hyperpolarization-activated cyclic nucleotide-gated (HCN) channels (Fig. 4C). *In vivo*, vestibular HCs acquire I_h postnatally. Its size increases dramatically at P3-P4 in the mouse utricle (Horwitz et al., 2010, 2011; Rüsch et al., 1998). We observed I_h in 22/34 (65%) Atoh1-nGFP$^+$ cells derived from vestibular tissue. None of the 32 cochlear-derived cells had detectable I_h (Fig. 4Ca), consistent with native cochlear HCs (Horwitz et al., 2010, 2011). This result suggests that only the vestibular progenitors were capable of becoming vestibular HCs.

Many HCs have an inwardly rectifying potassium current, I_{K1}, which contributes to setting a HC's resting membrane potential during development. Type I vestibular HCs express I_{K1} up to P4 and probably afterwards, whereas type II vestibular HCs express I_{K1} throughout the maturation process (Rüsch et al., 1998). Sixty percent (19/32) of the Atoh1-nGFP$^+$ vestibular-derived cells expressed I_{K1}: a fast inward current at the start of a hyperpolarizing voltage step, which rapidly deactivated after a depolarizing step (Fig. 4Cb). Within the cochlea, I_{K1} increases in size in IHCs from embryonic day (E) 15 to P12, the onset of hearing, then declines rapidly, disappearing by P15 (Marcotti et al., 2003a). It disappears from OHCs about a week earlier (Marcotti et al., 1999). In our experiments, I_{K1} was not detected in cochlear HC-like cells (Fig. 4Ac); they either never expressed I_{K1} or had passed through that stage of differentiation.

In vestibular-derived Atoh1$^+$ cells, large hyperpolarizing voltage steps evoked inward currents that followed a double-exponential time course reflecting the two components, I_{K1} and I_h (Fig. 4Cb). The faster time constant (0.99±0.32 ms, n=5) is comparable to values reported for I_{K1}, the fast inward rectifier, in early postnatal mouse utricular HCs (Rüsch et al., 1998). The slower time constant (92±21 ms, n=6) is comparable to the faster of two time constants for I_h activation in mouse utricular HCs (Horwitz et al., 2011); our 200-ms steps were too brief to substantially activate the slower I_h component.

In some hair cell-like cells, we recorded membrane voltage in current-clamp mode to assess the resting potential and voltage responses to injected current steps for comparison with the HC literature (Fig. 4D). The resting potentials for Atoh1$^+$ cells were −53±8 mV (four cochlear-derived cells) and −53±6 mV (six vestibular-derived cells). These values are set in large measure by K^+-selective inwardly rectifying and outwardly rectifying channels and are within the physiological range for postnatal HCs (Eatock and Hurley, 2003). Both cochlear-derived and vestibular-derived Atoh1$^+$ cells responded to current steps with voltage waveforms

Development (2016) 143, 4381-4393 doi:10.1242/dev.139840

within the normal range reported from postnatal HCs. We did not see the mixed Ca^{2+}-Na^{+} spikes that are typical of mouse IHCs in the first postnatal week (Marcotti et al., 2003b). All Atoh1^{+} cells lacked the voltage-gated Na^{+} currents of immature HC subtypes (Chabbert et al., 2003; Eckrich et al., 2012; Géléoc et al., 2004; Li et al., 2010; Marcotti et al., 2003b; Oliver et al., 1997; Witt et al., 1994; Wooltorton et al., 2007). Again, these channels either were never expressed or had stopped being expressed by the earliest time point we examined, 12 days of *in vitro* differentiation.

In all, our results support the hypothesis that the early postnatal inner ear harbors different populations of progenitors with limited differentiation capabilities. Organ-specific progenitors differentiated to Atoh1^{+} cells with many properties necessary for HC function, some of which are consistent with a relatively mature state: the presence and voltage dependence of delayed rectifiers in all cells; the lack of I_{Na} in all cells; the lack of Tmc2 and I_{K1} and the presence of prestin in cochlear cells; and the presence of I_{K1}, I_h and different kinds of outward rectifier in vestibular cells. Other mature properties – notably the distinctive negatively activating outward rectifiers of mature type I HCs and OHCs – failed to develop over the time frame examined.

Progenitor sub-populations

We next analyzed the potency of known HC progenitors within the cochlea. Lgr5 is expressed in inner border cells, inner pillar cells, and third row Deiters' cells (Chai et al., 2012; Shi et al., 2012) (Fig. 5A). Lgr5 was chosen as a marker to use for determining cell fates of neonatal progenitors. By crossing Lgr5-EGFP-IRES-CreER mice with floxed-tdTomato mice (Materials and Methods), we were able to trace the lineage of Lgr5^{+} cells in inner ear spheres (Fig. 5B) that we differentiated. After culture and differentiation, we observed that Lgr5^{+} lineage-traced cells could form HC-like cells, as indicated by

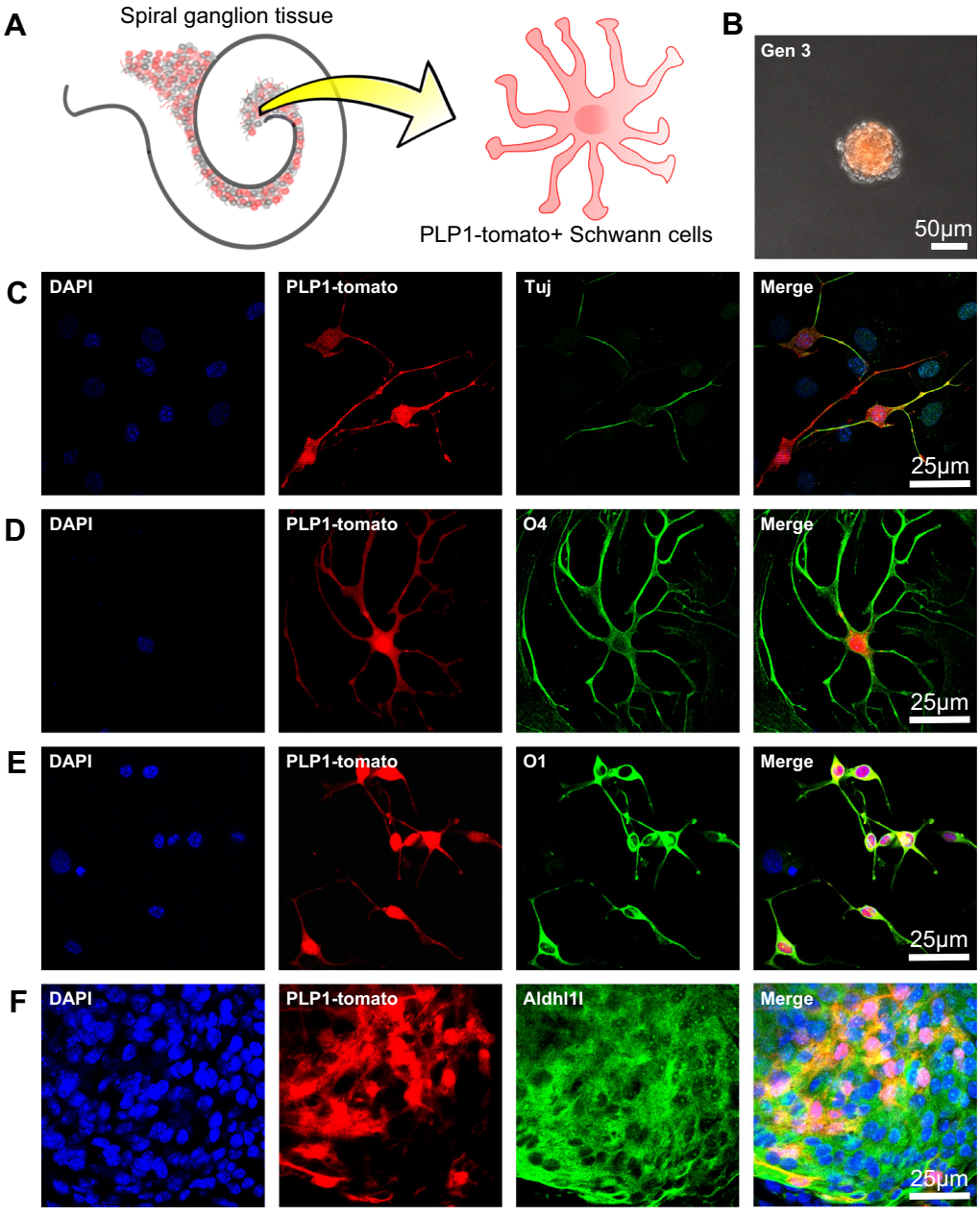

Fig. 6. Glial cells from the spiral ganglion are capable of producing neurons and CNS glia. (A) Glial cells (Schwann cells) were lineage traced using the PLP1-Cre-ERT mouse. (B) Glial cells (PLP1-tdTomato-positive, red) were maintained through three passages (generations, 'Gen') before differentiation. (C-F) Spiral ganglion-derived glial cells, labeled with tdTomato, were capable of giving rise to: neuron-like cells (C; immunoreactive for Tuj1, *n*=727 cells); immature non-myelinating oligodendrocytes (D; immunoreactive for O4, *n*=1299 cells); mature myelinating oligodendrocytes (E; immunoreactive for O1, *n*=1286 cells); and astrocytes (F; immunoreactive for Aldh1L1, *n*=531 cells).

Development (2016) 143, 4381-4393 doi:10.1242/dev.139840

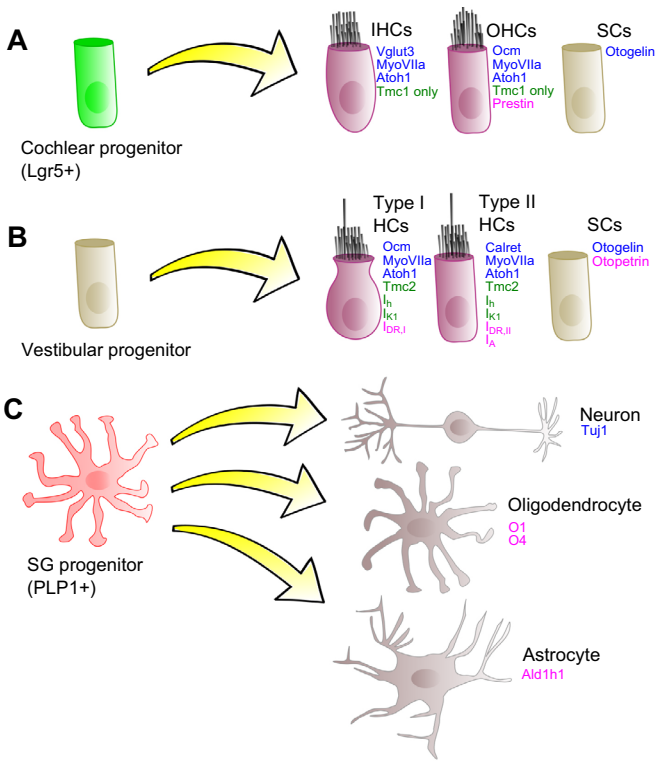

Fig. 7. Progenitor cells from the neonatal mouse inner ear showed different potency and differentiation capabilities. Single cells were expanded to form spheres, then differentiated by removing growth factors. (A) Lgr5$^+$ cochlear progenitor cells gave rise to inner (IHCs) and outer (OHCs) cochlear HCs and supporting cells (SCs) but not neurons. (B) Postnatal vestibular progenitor cells gave rise to vestibular type I and type II HCs and supporting cells. (C) Postnatal glial cells of the spiral ganglion (SG) became neurons and CNS glia in addition to Schwann cells. Markers and currents are shown according to the following hierarchy: blue, distinguishing between cell types within a tissue (organ of Corti, vestibular epithelia or spiral ganglion); green, distinguishing between two tissues; magenta, distinguishing both cell type and tissue type.

colocalization of myosin VIIA and tdTomato expression (n=20 cells; Fig. 5C). Myosin VIIA$^+$/tdTomato-negative cells were thought to result from incomplete recombination by this Cre (see Shi et al., 2013). To determine whether Lgr5$^+$ cells could also form neurons, we stained the differentiated cultures for Tuj1 (Tubb3), a tubulin that is highly specific to neurons (Fig. 5D). tdTomato was not colocalized with Tuj1 in any cells (n=696 Tuj1$^+$ cells), consistent with *in situ* data that localize Lgr5 to non-neuronal cells in the OC (Chai et al., 2012; Shi et al., 2012).

Because we had previously shown (Martinez-Monedero et al., 2008; Oshima et al., 2007) that neurons could differentiate from inner ear spheres, we set out to identify an inner ear progenitor that gives rise to neurons. We hypothesized that Schwann cells within the inner ear could be the source of the spheres from the spiral ganglion. Because these Schwann cells express PLP1 (Gomez-Casati et al., 2010), we crossed PLP1-Cre-ER mice with tdTomato mice and generated spheres from the spiral ganglion (Fig. 6A). The spiral ganglion comprises the cell bodies of cochlear afferents and Schwann cells, and only the Schwann cells are PLP1$^+$. In mature rodents, Schwann cells myelinate the peripheral processes of the bipolar spiral ganglion neurons, their cell bodies and the initial portions of their central axons (Hurley et al., 2007; Spoendlin, 1975; Toesca, 1996) up to the glia limitans, a transition zone near the cochlear nucleus where CNS glia (oligodendrocytes and astrocytes) take over the myelination (Hurley et al., 2007; Jalenques et al., 1995; Toesca, 1996; Valderrama-Canales et al., 1993).

The PLP1-tdTomato-positive progenitor cells gave rise to many labeled cells in third-generation spheres (Fig. 6B). We used PLP1 to mark spheres in an attempt to determine the potency of the progenitors in the newborn spiral ganglion. After differentiation of the third-generation spheres, we stained the cultures for specific markers of neurons and CNS glia to determine whether the PLP1$^+$ cells, which *in situ* would give rise to Schwann cells, also had the capacity to give rise to neurons and CNS glia. Co-staining of tdTomato and neuron-specific class III β-tubulin (n=727 cells; Fig. 6C) indicated that PLP1$^+$ glial cells formed neurons. We also observed co-staining of tdTomato and an antibody for the early-stage oligodendrocyte marker O4, a sulfated galactosylcerebroside on non-myelinating oligodendrocytes (Sommer and Schachner, 1981, 1982) (n=1299 cells; Fig. 6D). The PLP1$^+$ cells could also form more mature oligodendrocytes, as indicated by co-staining of tdTomato cells with antibody to O1, a galactocerebroside on terminally differentiated oligodendrocytes that are capable of myelination (Sommer and Schachner, 1981, 1982) (n=1286 cells, Fig. 6E). Lastly, co-staining of tdTomato and Aldh1L1, an aldehyde dehydrogenase that within the nervous system is highly specific to astrocytes (Cahoy et al., 2008) (n=531 cells; Fig. 6F), showed that the PLP1$^+$ cells could also form astrocytes. PLP1$^+$ cells in the differentiated cultures that lacked the markers Tuj1, O1 and O4 had probably differentiated as Schwann cells.

Thus, lineage-tracing experiments revealed that neonatal Schwann cells within the ganglion can form multiple cell types, including neuronal and glial cell types (oligodendrocyte-like and astrocyte-like). No myosin VIIA-expressing cells were observed after sphere differentiation (n=5 cultures), indicating that progenitor cells of the neonatal spiral ganglion did not differentiate into HC-like cells. Together, these methods, using combinations of markers and electrophysiological characteristics to distinguish cell type phenotype, could identify nine distinct cell types arising from the three compartments of the inner ear (Fig. 7).

DISCUSSION

The neonatal inner ear contains progenitor cells with the capacity to regenerate HCs after damage (Bramhall et al., 2014; Cox et al., 2014). The HCs regenerated in the cochlea, both spontaneously after damage or after Notch inhibition or Wnt pathway stimulation, arise from Lgr5$^+$ cells (Bramhall et al., 2014). Progenitor cells from the different inner ear compartments can be differentiated *in vitro* to cells that resemble HCs, neurons and glia (Martinez-Monedero et al., 2008; Oshima et al., 2007). HC-like cells derived from utricular progenitors resembled immature vestibular HCs in whole-cell recordings (Oshima et al., 2007), and progenitor-derived neurons had characteristics of auditory neurons (Martinez-Monedero et al., 2006). It was not determined whether these cell types arose from a common pluripotent stem cell, as reported previously (Li et al., 2003), or from multiple progenitor populations with more limited differentiation capacities. Because the sensory epithelia of the cochlear and vestibular organs are difficult to separate completely from neural elements, and because the cell types that arise from these different compartments show much overlap in gene expression, previous work had not allowed consensus to be met regarding the potency of potential inner ear progenitor cells (Liu et al., 2014). One paper concluded that cells in the mouse utricle were pluripotent (Li et al., 2003) and another that neurons and epithelial cells could be obtained from epithelial compartments (Oshima et al., 2007). Knowing which progenitor

Development (2016) 143, 4381-4393 doi:10.1242/dev.139840

cells give rise to which cell types is of fundamental interest and also may be necessary for the regeneration of inner ear cells for therapeutic use.

Numerous studies of inner ear development show that the otic placode is the source of both neural and sensory elements of the adult ear (Barald and Kelley, 2004; Kelley, 2006; Raft and Groves, 2015), and the placode probably contains progenitor cells that divide and become specified to neural and sensory fates. The otic placode gives rise to the otocyst in the early stages of inner ear morphogenesis, and the otocyst becomes regionalized into areas that eventually form the cochlea and vestibular organs (Barald and Kelley, 2004; Fekete and Wu, 2002; Groves and Fekete, 2012; Raft and Groves, 2015), both of which arise from the prosensory epithelium. In the mouse inner ear, the neural lineage separates from the sensory lineage at E9.5 (Ma et al., 1998), when the neuroblasts delaminate from the prosensory region. These proneural cells are infiltrated by cells of the neural crest that give rise to the glia of the inner ear (Breuskin et al., 2010; D'Amico-Martel and Noden, 1983). Thus, the compartments that we study here contain progenitors from both neural crest and otic placode and generate specialized cell types including neurons, glia and sensory cells.

Progenitor cell markers are widely expressed in the embryo and become restricted to populations of progenitors as development proceeds. Thus, the time at which progenitors in the developing cochlea or utricle are labeled for lineage determination is important for the pattern of labeling. Here, we show that activation of Cre for labeling of mouse inner ear progenitor cells at neonatal time points reveals three distinct populations: $Lgr5^+$ cochlear progenitors, $Lgr5^+$ vestibular progenitors and $PLP1^+$ Schwann cell derivatives.

Knowledge of the differentiation capacity of closely related and physically overlapping progenitor cell populations is important for an understanding of their functional role in generating the multiple cell types that comprise a complex tissue. The plasticity of neural progenitors has been followed during regionalization of the fore-, mid- and hindbrain (Hitoshi et al., 2002; Shen et al., 2006). These studies show an increasing level of regionalization, as fewer specified stem cells mature into more highly determined progenitors and migrate into their final positions. Cortical neurons are derived from distinct progenitor cells during development (Tyler et al., 2015). The fate of the progenitors is partially pre-programmed for broad regional identity and partly determined by inductive cues as the progenitors assume their identity (Gage, 2002; Hitoshi et al., 2002; Shen et al., 2006; Zhao et al., 2008). Some of the neural progenitors in the embryo are restricted to playing a developmental role only. Stem cells remain, however, in the dentate gyrus and the subventricular zone, where they give rise to the rostral migratory stream and hippocampal neurons (Kempermann et al., 2015; Kriegstein and Alvarez-Buylla, 2009; Zhao et al., 2008). The capacity of neural stem cells to differentiate to single or multiple cell types has been difficult to assess without sufficient markers for both the progenitors and their cellular progeny.

The neural crest bears considerable resemblance to the placodes containing the stem cells that generate the sensory ganglia of the inner ear. Both give rise to multiple cell types, including glutamatergic sensory neurons as well as peripheral and central glia. Adult dorsal root ganglion (DRG), like adult spiral ganglion, gives rise to neurospheres (Li et al., 2007). However, neural crest-derived progenitor cells in DRGs maintain their regenerative capacity into adulthood, unlike what has been observed to date in spiral ganglion. DRG cells divide in response to damage and differentiate into neurons at the site of injury (Gallaher et al., 2014; Li et al., 2007).

Understanding the postnatal capacity for regeneration is particularly relevant to poorly regenerating tissues. In the inner ear, well-defined compartments and considerable existing data on cell-specific proteins and electrophysiological phenotypes make this goal achievable. We used a previously identified marker (Lgr5) to trace the lineage of specific OC progenitors. Although the mature cochlear epithelium has little regenerative capacity, early postnatal $Lgr5^+$ cells show an ability to both divide and differentiate to HCs. We identified a new marker (PLP1) for spiral ganglion progenitors, which we also lineage traced. The $PLP1^+$ Schwann cells also show some capacity for cell division in the adult (Lang et al., 2011). We observed the development of distinct HC, neural and glial subtypes from neonatal progenitors from the different inner ear compartments, suggesting that the differentiation capacity of postnatal inner ear progenitors is limited to cells of the originating tissue (Fig. 7).

The newly created HC-like cells expressed many genes necessary for proper function. In addition to demonstrating immunoreactivity for proteins key to HC-specific functions and morphological characteristics (prestin, espin, oncomodulin and PMCA2), we showed that the newly created cells expressed species of mRNA that are necessary for mechanotransduction, bundle structure, synaptic function and Ca^{2+} buffering. Interestingly, differentiated cochlear cells showed robust prestin expression, a characteristic of OHCs near the onset of hearing (Belyantseva et al., 2000). Similarly, HC-like cells differentiated from the cochlea only expressed the transduction channel-associated gene family member TMC1, whereas vestibular cells expressed both TMC1 and TMC2. This resembles the expression pattern in mature HCs within native tissue (Kawashima et al., 2011; Pan et al., 2013). We also observed that newly created HC-like cells acquired the physiological behavior of bona fide HCs, such as resting potentials around −55 mV, large outwardly rectifying currents probably carried by K^+, and, in cells from vestibular tissue, additional currents (I_{KA}, I_h and I_{K1}) that occur frequently in mature native vestibular cells. These gene expression and physiological results are consistent with results from native postnatal HCs beyond the earliest stages of differentiation. It seems likely that immature HC characteristics would have been observed at earlier stages (<12 days) following the start of differentiating culture conditions, but we did not study that period because at early stages the levels of GFP, our marker for *Atoh1* expression, were low.

Atoh1 overexpression *in situ* causes trans-differentiation of supporting cells to ectopic HCs, which have been called 'primordial' because their properties do not depend on the organ in which they reside (Yang et al., 2012). In our method, the expression of *Atoh1* was influenced by passive signaling stimulated by removal of growth factors, and a given inner ear organ generated its own HC subtypes. Endogenous signaling within the progenitor cell population of each organ may give rise to cell types more representative of the differentiation capacity of each tissue. Production of HCs can be induced by Wnt activation (Shi et al., 2013, 2014) or Notch inhibition (Doetzlhofer et al., 2009; Mizutari et al., 2013; Pan et al., 2010; Yamamoto et al., 2006). Notch-mediated lateral inhibition (Daudet and Lewis, 2005; Lanford et al., 1999) and innate Wnt signaling are both crucial for the development of HCs (Shi et al., 2013, 2014). The Wnt pathway interacts with the Notch pathway in development (Collu et al., 2014; Shi et al., 2010) and this interaction could regulate the level of expression of *Atoh1* and other genes. Bypassing key components of developmental pathways via viral *Atoh1* transduction might disrupt mechanisms that control levels of Wnt and Notch factors and thus create 'primordial' HCs.

Development (2016) 143, 4381-4393 doi:10.1242/dev.139840

Previous work established that neonatal inner ear tissues can generate both HCs and neurons, but the potency of individual progenitor cells was not established. Our work shows that in the neonatal mouse, HC progenitors and neural progenitors are different populations with different potencies. The cochlea-derived Lgr5-expressing cells produced HC-like cells, consistent with previous work (Chai et al., 2012; Shi et al., 2013, 2012), but did not produce neural cell types. We demonstrated that PLP1-expressing glial cells from the neonatal spiral ganglion were capable of differentiating both to neurons and to multiple forms of glia that are outside the otic lineage. CNS cell types (oligodendrocytes) were also seen after differentiation of DRG neurospheres (Binder et al., 2011). Although bipotent, the PLP1$^+$ cells in our study did not give rise to HCs, just as Lgr5$^+$ cells did not give rise to neurons. This is an important observation for efforts to regenerate both HCs and neurons. Identification of these distinct progenitor compartments is an important step in fate mapping of the inner ear, although we cannot rule out the existence of other lineages. Thus, the cochlea, vestibular organs and spiral ganglion progenitor cells in mice are partly committed to specific cell fates even at birth. Neural progenitor cells in the inner ear of neonatal mice give rise to a greater range of cell types than do HC progenitors but both have limited potency. This work advances our understanding of the commitment of tissue stem cells to cell fates of the mammalian inner ear.

MATERIALS AND METHODS

Isolation of progenitor cells from the inner ear

We extracted progenitor cells from the neonatal mouse inner ear of several mouse lines (Table S1). All animal studies were conducted under an approved institutional protocol according to National Institutes of Health guidelines.

For each experiment, the otic capsules of six to eight mice (age range P1-4) were carefully extracted from the skull and any brain tissue was discarded. The cochleas and vestibular organs (utricle, saccule and ampullas combined) were dissected out (Fig. 1) in HBSS and kept separate from each other for the remainder of the protocol, allowing us to analyze the developmental properties of each tissue separately. For cochleas, the OC (sensory epithelium) was separated from the stria vascularis (ion transport epithelium) and the bony modiolus, which houses the spiral ganglion, comprising the cell bodies of auditory nerve fibers and associated Schwann cells (Fig. 1).

The OC and vestibular organs were transferred to the dissociating medium TrypLE (Life Technologies) for 11-13 min at 37°C and then dissociated by trituration with a pipette. The triturated cells were passed through a 70-µm cell strainer to remove tissue and bone debris. Single cells were deposited in ultralow-cluster plates (Corning) and proliferated to produce floating spheres by culturing for several days in a 1:1 mixture of DMEM/high-glucose medium and F12, supplemented with N2, B27 (Life Technologies), EGF (20 ng/ml; Chemicon), bFGF (10 ng/ml; Chemicon), IGF-1 (50 ng/ml; Chemicon) and heparan sulfate (50 ng/ml; Sigma-Aldrich). The spheres were passaged by trituration with a 100-µl pipette, then placed in fresh culture medium. For each experiment, spheres were passaged three times at intervals of 3-4 days to eliminate HCs or neurons from the original tissue.

Mouse strains for lineage tracing

We analyzed the potency of Lgr5$^+$ cells from the OC and PLP1$^+$ cells from the spiral ganglion. Male Lgr5-EGFP-IRES-Cre-ER (jaxmice.jax.org/strain/008875.html) and male PLP1-Cre-ER mice (jaxmice.jax.org/strain/005975.html) were crossed with female tdTomato reporter mice (jaxmice.jax.org/strain/007909.html) in order to lineage trace the cells that resulted from each cell type. Mother mice were injected with 600 µl tamoxifen (50 mg/ml) on the day of birth (P0) and P1. Pups were dissected at P3 and were identified as positive or negative for the marker of interest based on cellular fluorescence. Spheres were generated from the OC of Lgr5$^+$ mice and the modiolar tissue (containing the spiral ganglion, including cochlear neuronal cell bodies and glial cells) of PLP1$^+$ mice.

Differentiation and treatment of spheres

To generate differentiated cells, third-generation spheres were plated in 4-well plates (Greiner, Austria) on round 10-mm glass coverslips coated with poly-L-lysine (Trevigen). Attachment took place overnight in DMEM-high glucose/F12 (mixed 1:1, Life Technologies) containing N2 and B27 (Invitrogen); the elimination of growth factors halted cell division and promoted differentiation. Spheres were differentiated in these conditions for 7-70 days, with fresh culture medium applied every 2-3 days to maintain optimal culture conditions. Cells were then harvested for RT-PCR (to analyze gene expression), immunostaining (to identify and count differentiated cells expressing proteins characteristic of specific cell types) or whole-cell patch clamping (to test for functional maturation and expression of voltage-dependent properties that differentiate cochlear and vestibular sensory cells).

RT-PCR

We used RT-PCR to analyze gene expression. RNA was extracted from the inner ears of P5 CD1 mice or from differentiated spheres, using the RNeasy Maxi Kit (Qiagen) according to the manufacturer's instructions, denatured at 65°C for 5 min, and reverse-transcribed using ImProm II (Promega) and random hexamer primers. The reverse transcription conditions were 25°C for 5 min followed by 42°C for 60 min, and the reaction was terminated at 70°C for 15 min. To the resulting cDNA we added primers (Table S2) for various inner ear proteins. The primers were taken from PrimerBank (pga.mgh.harvard.edu/primerbank) or designed with Primer3 (bioinfo.ut.ee/primer3) and, where possible, were intron-spanning to preclude amplification of genomic DNA. The amplified products were then separated on a 2% agarose gel, stained with ethidium bromide, and visualized under a UV transilluminator. Spheres at the third generation were assessed for expression of myosin VIIa in the absence of differentiation (Fig. S1). Lanes with *Gapdh* primers and water were run as positive controls for the tissue and negative controls for contamination, respectively.

Immunohistochemistry

We used immunohistochemistry to identify and count differentiated cells that expressed proteins characteristic of specific cell types. Differentiated spheres were fixed at room temperature in 4% paraformaldehyde/PBS for 15-20 min, washed in PBS, permeabilized and blocked for 1 h in blocking solution (0.3% Triton X-100 and 15% heat-inactivated goat or donkey serum in PBS), and exposed to diluted primary antibody (in 0.1% Triton X-100 and 10% heat-inactivated goat or donkey serum in PBS) overnight at 4°C. Primary antibodies, their target proteins, and antibody dilutions are listed in Table S3. Secondary antibodies (AlexaFluor 488, 568 and 647 conjugated; Invitrogen) were diluted 1:500 for detection of primary antibodies. Nuclei were visualized with 4,6-diamidino-2-phenylindole (DAPI; Vector Laboratories). Staining was visualized by confocal microscopy (TCD, Leica). All cellular counts of gene expression were performed manually.

Electrophysiology

We used the patch clamp method to record whole-cell currents and voltages from differentiating cells to test for functional maturation and expression of voltage-dependent properties that differentiate cochlear and vestibular sensory cells. Prior to recording, the cell culture solution was replaced with L-15 (Leibowitz 15) medium (supplemented with 10 mM HEPES, pH 7.3, ~320 mmol/kg). Recordings were made at room temperature (22-25°C). The pipette solution contained (in mM): 135 KCl, 3.5 $MgCl_2$, 5 Na_2ATP, 10 HEPES, 10 EGTA, 0.1 Na-cAMP, 0.1 Li-GTP; pH was adjusted to 7.4 by adding 15 mM KOH; 280±5 mmol/kg. Recording pipettes were pulled from borosilicate glass and heat polished to a resistance of 3-9 MΩ.

Currents were recorded with a patch-clamp amplifier (Axopatch 200B or Multiclamp 700; Molecular Devices). Series resistance (R_S) was compensated 20-90% with the intrinsic circuitry of the amplifier. Currents

Development (2016) 143, 4381-4393 doi:10.1242/dev.139840

were filtered with an eight-pole low-pass Bessel filter with a corner frequency of 2 kHz and sampled at more than twice the filter frequency with a Digidata 1440 board (Molecular Devices), controlled by Clampex software (version 10.1; Molecular Devices).

Analyses and fits were performed with Origin software (version 9; OriginLab Software). All cells considered for analysis had >100 MΩ input resistance. To obtain the voltage dependence of activation (activation curve) for a current, we stepped through an iterated series of test potentials and measured the tail current at −40 mV, i.e. the current immediately upon stepping to −40 mV after each test step. Plotting tail current against test-step voltage produced sigmoidal activation curves, which show how the conductance depends on voltage. Activation curves were fit with a Boltzmann function (Eqn 1), where $I(V)$ is current at voltage V, I_{min} and I_{max} are minimum and maximum currents, $V_{1/2}$ is voltage at half-maximal activation, and S is the voltage change corresponding to an e-fold increase in I:

$$I(V) = \frac{I_{max} - I_{min}}{1 + \exp[(V_{1/2} - V)/S]} + I_{min}. \quad (1)$$

The time course of current activation was fit with a mono-exponential decay function. Averaged values are presented as mean±s.e.m.

Acknowledgements

We thank Dr Judith Kempfle for help and guidance throughout the project, and Drs Jeff Holt, David Breault and John Rosowski for their thoughtful input on experiments and analysis.

Competing interests

The authors declare no competing or financial interests.

Author contributions

Designed research: W.J.M., R.A.E., A.S.B.E.; Performed research: W.J.M., D.T.M.; Analyzed data: W.J.M., R.A.E., A.S.B.E.; Wrote the paper: W.J.M., R.A.E., A.S.B.E. All authors read and revised the paper.

Funding

This work was supported by the National Institute on Deafness and Other Communication Disorders [DC002290 and DC012347 to R.A.E., DC007174 to A.S.B.E.]; and by a cooperative grant from the European Commission (FP7 Health 2013 Innovation). Deposited in PMC for release after 12 months.

Supplementary information

Supplementary information available online at
http://dev.biologists.org/lookup/doi/10.1242/dev.139840.supplemental

References

Agrawal, Y., Carey, J. P., Della Santina, C. C., Schubert, M. C. and Minor, L. B. (2009). Disorders of balance and vestibular function in US adults: data from the National Health and Nutrition Examination Survey, 2001-2004. *Arch. Intern. Med.* **169**, 938-944.

Barald, K. F. and Kelley, M. W. (2004). From placode to polarization: new tunes in inner ear development. *Development* **131**, 4119-4130.

Belyantseva, I. A., Adler, H. J., Curi, R., Frolenkov, G. I. and Kachar, B. (2000). Expression and localization of prestin and the sugar transporter GLUT-5 during development of electromotility in cochlear outer hair cells. *J. Neurosci.* **20**, RC116.

Barker, N., van Es, J. H., Kuipers, J., Kujala, P., van den Born, M., Cozijnsen, M., Haegebarth, A., Korving, J., Begthel, H., Peters, P. J. and Clevers, H. (2007). Identification of stem cells in small intestine and colon by marker gene Lgr5. *Nature* **25**, 1003-1007.

Bermingham, N. A., Hassan, B. A., Price, S. D., Vollrath, M. A., Ben-Arie, N., Eatock, R. A., Bellen, H. J., Lysakowski, A. and Zoghbi, H. Y. (1999). Math1: an essential gene for the generation of inner ear hair cells. *Science* **284**, 1837-1841.

Binder, E., Rukavina, M., Hassani, H., Weber, M., Nakatani, H., Reiff, T., Parras, C., Taylor, V. and Rohrer, H. (2011). Peripheral nervous system progenitors can be reprogrammed to produce myelinating oligodendrocytes and repair brain lesions. *J. Neurosci.* **31**, 6379-6391.

Bramhall, N. F., Shi, F., Arnold, K., Hochedlinger, K. and Edge, A. S. B. (2014). Lgr5-positive supporting cells generate new hair cells in the postnatal cochlea. *Stem Cell Rep.* **2**, 311-322.

Breuskin, I., Bodson, M., Thelen, N., Thiry, M., Borgs, L., Nguyen, L., Stolt, C., Wegner, M., Lefebvre, P. P. and Malgrange, B. (2010). Glial but not neuronal development in the cochleo-vestibular ganglion requires Sox10. *J. Neurochem.* **114**, 1827-1839.

Burns, J. C. and Corwin, J. T. (2014). Responses to cell loss become restricted as the supporting cells in mammalian vestibular organs grow thick junctional actin bands that develop high stability. *J. Neurosci.* **34**, 1998-2011.

Burns, J. C., Cox, B. C., Thiede, B. R., Zuo, J. and Corwin, J. T. (2012). In vivo proliferative regeneration of balance hair cells in newborn mice. *J. Neurosci.* **32**, 6570-6577.

Cahoy, J. D., Emery, B., Kaushal, A., Foo, L. C., Zamanian, J. L., Christopherson, K. S., Xing, Y., Lubischer, J. L., Krieg, P. A., Krupenko, S. A. et al. (2008). A transcriptome database for astrocytes, neurons, and oligodendrocytes: a new resource for understanding brain development and function. *J. Neurosci.* **28**, 264-278.

Chabbert, C., Mechaly, I., Sieso, V., Giraud, P., Brugeaud, A., Lehouelleur, J., Couraud, F., Valmier, J. and Sans, A. (2003). Voltage-gated Na+ channel activation induces both action potentials in utricular hair cells and brain-derived neurotrophic factor release in the rat utricle during a restricted period of development. *J. Physiol.* **553**, 113-123.

Chai, R., Kuo, B., Wang, T., Liaw, E. J., Xia, A., Jan, T. A., Liu, Z., Taketo, M. M., Oghalai, J. S., Nusse, R. et al. (2012). Wnt signaling induces proliferation of sensory precursors in the postnatal mouse cochlea. *Proc. Natl. Acad. Sci. USA* **109**, 8167-8172.

Chen, Q., Mahendrasingam, S., Tickle, J. A., Hackney, C. M., Furness, D. N. and Fettiplace, R. (2012). The development, distribution and density of the plasma membrane calcium ATPase 2 calcium pump in rat cochlear hair cells. *Eur. J. Neurosci.* **36**, 2302-2310.

Collu, G. M., Hidalgo-Sastre, A. and Brennan, K. (2014). Wnt-Notch signalling crosstalk in development and disease. *Cell. Mol. Life Sci.* **71**, 3553-3567.

Cox, B. C., Chai, R., Lenoir, A., Liu, Z., Zhang, L., Nguyen, D.-H., Chalasani, K., Steigelman, K. A., Fang, J., Rubel, E. W. et al. (2014). Spontaneous hair cell regeneration in the neonatal mouse cochlea in vivo. *Development* **141**, 816-829.

D'Amico-Martel, A. and Noden, D. M. (1983). Contributions of placodal and neural crest cells to avian cranial peripheral ganglia. *Am. J. Anat.* **166**, 445-468.

Daudet, N. and Lewis, J. (2005). Two contrasting roles for Notch activity in chick inner ear development: specification of prosensory patches and lateral inhibition of hair-cell differentiation. *Development* **132**, 541-551.

de Lau, W., Barker, N., Low, T. Y., Koo, B.-K., Li, V. S. W., Teunissen, H., Kujala, P., Haegebarth, A., Peters, P. J., van de Wetering, M. et al. (2011). Lgr5 homologues associate with Wnt receptors and mediate R-spondin signalling. *Nature* **476**, 293-297.

Dechesne, C. J., Rabejac, D. and Desmadryl, G. (1994). Development of calretinin immunoreactivity in the mouse inner ear. *J. Comp. Neurol.* **346**, 517-529.

Desai, S. S., Zeh, C. and Lysakowski, A. (2005). Comparative morphology of rodent vestibular periphery. I. Saccular and utricular maculae. *J. Neurophysiol.* **93**, 251-266.

Doetzlhofer, A., Basch, M. L., Ohyama, T., Gessler, M., Groves, A. K. and Segil, N. (2009). Hey2 regulation by FGF provides a Notch-independent mechanism for maintaining pillar cell fate in the organ of Corti. *Dev. Cell* **16**, 58-69.

Dou, H., Vazquez, A. E., Namkung, Y., Chu, H., Cardell, E. L., Nie, L., Parson, S., Shin, H.-S. and Yamoah, E. N. (2004). Null mutation of alpha1D Ca2+ channel gene results in deafness but no vestibular defect in mice. *J. Assoc. Res. Otolaryngol.* **5**, 215-226.

Dumont, R. A., Lins, U., Filoteo, A. G., Penniston, J. T., Kachar, B. and Gillespie, P. G. (2001). Plasma membrane Ca2+-ATPase isoform 2a is the PMCA of hair bundles. *J. Neurosci.* **21**, 5066-5078.

Eatock, R. A. and Hurley, K. M. (2003). Functional development of hair cells. *Curr. Top. Dev. Biol.* **57**, 389-448.

Eckrich, T., Varakina, K., Johnson, S. L., Franz, C., Singer, W., Kuhn, S., Knipper, M., Holley, M. C. and Marcotti, W. (2012). Development and function of the voltage-gated sodium current in immature mammalian cochlear inner hair cells. *PLoS ONE* **7**, e45732.

El-Amraoui, A., Cohen-Salmon, M., Petit, C. and Simmler, M.-C. (2001). Spatiotemporal expression of otogelin in the developing and adult mouse inner ear. *Hear. Res.* **158**, 151-159.

Elgoyhen, A. B. and Franchini, L. F. (2011). Prestin and the cholinergic receptor of hair cells: positively-selected proteins in mammals. *Hear. Res.* **273**, 100-108.

Fekete, D. M. and Wu, D. K. (2002). Revisiting cell fate specification in the inner ear. *Curr. Opin. Neurobiol.* **12**, 35-42.

Fuentealba, L. C., Rompani, S. B., Parraguez, J. I., Obernier, K., Romero, R., Cepko, C. L. and Alvarez-Buylla, A. (2015). Embryonic origin of postnatal neural stem cells. *Cell* **161**, 1644-1655.

Gage, F. H. (2002). Neurogenesis in the adult brain. *J. Neurosci.* **22**, 612-613.

Gallaher, Z. R., Johnston, S. T. and Czaja, K. (2014). Neural proliferation in the dorsal root ganglia of the adult rat following capsaicin-induced neuronal death. *J. Comp. Neurol.* **522**, 3295-3307.

Géléoc, G. S. G., Risner, J. R. and Holt, J. R. (2004). Developmental acquisition of voltage-dependent conductances and sensory signaling in hair cells of the embryonic mouse inner ear. *J. Neurosci.* **24**, 11148-11159.

Gillespie, P. G. (2004). Myosin I and adaptation of mechanical transduction by the inner ear. *Philos. Trans. R. Soc. Lond. B Biol. Sci.* **359**, 1945-1951.

Gomez-Casati, M. E., Murtie, J. C., Rio, C., Stankovic, K., Liberman, M. C. and Corfas, G. (2010). Nonneuronal cells regulate synapse formation in the vestibular

sensory epithelium via erbB-dependent BDNF expression. *Proc. Natl. Acad. Sci. USA* **107**, 17005-17010.
Grati, M. and Kachar, B. (2011). Myosin VIIa and sans localization at stereocilia upper tip-link density implicates these Usher syndrome proteins in mechanotransduction. *Proc. Natl. Acad. Sci. USA* **108**, 11476-11481.
Groves, A. K. and Fekete, D. M. (2012). Shaping sound in space: the regulation of inner ear patterning. *Development* **139**, 245-257.
Groves, A. K., Zhang, K. D. and Fekete, D. M. (2013). The genetics of hair cell development and regeneration. *Annu. Rev. Neurosci.* **36**, 361-381.
Hasson, T., Heintzelman, M. B., Santos-Sacchi, J., Corey, D. P. and Mooseker, M. S. (1995). Expression in cochlea and retina of myosin VIIa, the gene product defective in Usher syndrome type 1B. *Proc. Natl. Acad. Sci. USA* **92**, 9815-9819.
Hill, J. K., Williams, D. E., LeMasurier, M., Dumont, R. A., Strehler, E. E. and Gillespie, P. G. (2006). Splice-site A choice targets plasma-membrane Ca2 +-ATPase isoform 2 to hair bundles. *J. Neurosci.* **26**, 6172-6180.
Hitoshi, S., Tropepe, V., Ekker, M. and van der Kooy, D. (2002). Neural stem cell lineages are regionally specified, but not committed, within distinct compartments of the developing brain. *Development* **129**, 233-244.
Holt, J. R., Vollrath, M. A. and Eatock, R. A. (1999). Stimulus processing by type II hair cells in the mouse utricle. *Ann. N. Y. Acad. Sci.* **871**, 15-26.
Holt, J. R., Gillespie, S. K. H., Provance, D. W., Shah, K., Shokat, K. M., Corey, D. P., Mercer, J. A. and Gillespie, P. G. (2002). A chemical-genetic strategy implicates myosin-1c in adaptation by hair cells. *Cell* **108**, 371-381.
Horwitz, G. C., Lelli, A., Géléoc, G. S. G. and Holt, J. R. (2010). HCN channels are not required for mechanotransduction in sensory hair cells of the mouse inner ear. *PLoS ONE* **5**, e8627.
Horwitz, G. C., Risner-Janiczek, J. R., Jones, S. M. and Holt, J. R. (2011). HCN channels expressed in the inner ear are necessary for normal balance function. *J. Neurosci.* **31**, 16814-16825.
Hurley, P. A., Crook, J. M. and Shepherd, R. K. (2007). Schwann cells revert to non-myelinating phenotypes in the deafened rat cochlea. *Eur. J. Neurosci.* **26**, 1813-1821.
Jalenques, I., Albuisson, E., Despres, G. and Romand, R. (1995). Distribution of glial fibrillary acidic protein (GFAP) in the cochlear nucleus of adult and aged rats. *Brain Res.* **686**, 223-232.
Kanzaki, S., Beyer, L. A., Canlon, B., Meixner, W. M. and Raphael, Y. (2002). The cytocaud: a hair cell pathology in the waltzing Guinea pig. *Audiol. Neurootol.* **7**, 289-297.
Kawashima, Y., Géléoc, G. S. G., Kurima, K., Labay, V., Lelli, A., Asai, Y., Makishima, T., Wu, D. K., Della Santina, C. C., Holt, J. R. et al. (2011). Mechanotransduction in mouse inner ear hair cells requires transmembrane channel-like genes. *J. Clin. Invest.* **121**, 4796-4809.
Kazmierczak, P., Sakaguchi, H., Tokita, J., Wilson-Kubalek, E. M., Milligan, R. A., Müller, U. and Kachar, B. (2007). Cadherin 23 and protocadherin 15 interact to form tip-link filaments in sensory hair cells. *Nature* **449**, 87-91.
Kelley, M. W. (2006). Regulation of cell fate in the sensory epithelia of the inner ear. *Nat. Rev. Neurosci.* **7**, 837-849.
Kempermann, G., Song, H. and Gage, F. H. (2015). Neurogenesis in the Adult Hippocampus. *Cold Spring Harb. Perspect. Biol.* **7**, a018812.
Kim, E., Hyrc, K. L., Speck, J., Lundberg, Y. W., Salles, F. T., Kachar, B., Goldberg, M. P., Warchol, M. E. and Ornitz, D. M. (2010). Regulation of cellular calcium in vestibular supporting cells by otopetrin 1. *J. Neurophysiol.* **104**, 3439-3450.
Kriegstein, A. and Alvarez-Buylla, A. (2009). The glial nature of embryonic and adult neural stem cells. *Annu. Rev. Neurosci.* **32**, 149-184.
Kujawa, S. G. and Liberman, M. C. (2009). Adding insult to injury: cochlear nerve degeneration after 'temporary' noise-induced hearing loss. *J. Neurosci.* **29**, 14077-14085.
Lanford, P. J., Lan, Y., Jiang, R., Lindsell, C., Weinmaster, G., Gridley, T. and Kelley, M. W. (1999). Notch signalling pathway mediates hair cell development in mammalian cochlea. *Nat. Genet.* **21**, 289-292.
Lang, H., Li, M., Kilpatrick, L. A., Zhu, J., Samuvel, D. J., Krug, E. L. and Goddard, J. C. (2011). Sox2 up-regulation and glial cell proliferation following degeneration of spiral ganglion neurons in the adult mouse inner ear. *J. Assoc. Res. Otolaryngol.* **12**, 151-171.
Li, H., Liu, H. and Heller, S. (2003). Pluripotent stem cells from the adult mouse inner ear. *Nat. Med.* **9**, 1293-1299.
Li, H.-Y., Say, E. H. M. and Zhou, X.-F. (2007). Isolation and characterization of neural crest progenitors from adult dorsal root ganglia. *Stem Cells* **25**, 2053-2065.
Li, A., Xue, J. and Peterson, E. H. (2008). Architecture of the mouse utricle: macular organization and hair bundle heights. *J. Neurophysiol.* **99**, 718-733.
Li, G. Q., Meredith, F. L. and Rennie, K. J. (2010). Development of K^+ and Na^+ conductances in rodent postnatal semicircular canal type I hair cells. *Am. J. Physiol. Regul. Integr. Comp. Physiol.* **298**, R351-R358.
Liu, Q., Chen, P. and Wang, J. (2014). Molecular mechanisms and potentials for differentiating inner ear stem cells into sensory hair cells. *Dev. Biol.* **390**, 93-101.
Lumpkin, E. A., Collisson, T., Parab, P., Omer-Abdalla, A., Haeberle, H., Chen, P., Doetzlhofer, A., White, P., Groves, A., Segil, N. et al. (2003). Math1-driven GFP expression in the developing nervous system of transgenic mice. *Gene Expr. Patterns* **3**, 389-395.
Luo, L., Bennett, T., Jung, H. H. and Ryan, A. F. (1998). Developmental expression of alpha 9 acetylcholine receptor mRNA in the rat cochlea and vestibular inner ear. *J. Comp. Neurol.* **393**, 320-331.
Ma, Q., Chen, Z., del Barco Barrantes, I., de la Pompa, J. L. and Anderson, D. J. (1998). neurogenin1 is essential for the determination of neuronal precursors for proximal cranial sensory ganglia. *Neuron* **20**, 469-482.
Malgrange, B., Belachew, S., Thiry, M., Nguyen, L., Rogister, B., Alvarez, M.-L., Rigo, J.-M., Van De Water, T. R., Moonen, G. and Lefebvre, P. P. (2002). Proliferative generation of mammalian auditory hair cells in culture. *Mech. Dev.* **112**, 79-88.
Marcotti, W., Géléoc, G. S. G., Lennan, G. W. T. and Kros, C. J. (1999). Transient expression of an inwardly rectifying potassium conductance in developing inner and outer hair cells along the mouse cochlea. *Pflugers Arch.* **439**, 113-122.
Marcotti, W., Johnson, S. L., Holley, M. C. and Kros, C. J. (2003a). Developmental changes in the expression of potassium currents of embryonic, neonatal and mature mouse inner hair cells. *J. Physiol.* **548**, 383-400.
Marcotti, W., Johnson, S. L., Rüsch, A. and Kros, C. J. (2003b). Sodium and calcium currents shape action potentials in immature mouse inner hair cells. *J. Physiol.* **552**, 743-761.
Martinez-Monedero, R., Corrales, C. E., Cuajungco, M. P., Heller, S. and Edge, A. S. B. (2006). Reinnervation of hair cells by auditory neurons after selective removal of spiral ganglion neurons. *J. Neurobiol.* **66**, 319-331.
Martinez-Monedero, R., Yi, E., Oshima, K., Glowatzki, E. and Edge, A. S. B. (2008). Differentiation of inner ear stem cells to functional sensory neurons. *Dev. Neurobiol.* **68**, 669-684.
Mizutari, K., Fujioka, M., Hosoya, M., Bramhall, N., Okano, H. J., Okano, H. and Edge, A. S. B. (2013). Notch inhibition induces cochlear hair cell regeneration and recovery of hearing after acoustic trauma. *Neuron* **77**, 58-69.
Ogata, Y. and Slepecky, N. B. (1995). Immunocytochemical comparison of posttranslationally modified forms of tubulin in the vestibular end-organs of the gerbil: tyrosinated, acetylated and polyglutamylated tubulin. *Hear. Res.* **86**, 125-131.
Oliver, D., Plinkert, P., Zenner, H. P. and Ruppersberg, J. P. (1997). Sodium current expression during postnatal development of rat outer hair cells. *Pflugers Arch.* **434**, 772-778.
Oshima, K., Grimm, C. M., Corrales, C. E., Senn, P., Martinez Monedero, R., Géléoc, G. S. G., Edge, A., Holt, J. R. and Heller, S. (2007). Differential distribution of stem cells in the auditory and vestibular organs of the inner ear. *J. Assoc. Res. Otolaryngol.* **8**, 18-31.
Pan, W., Jin, Y., Stanger, B. and Kiernan, A. E. (2010). Notch signaling is required for the generation of hair cells and supporting cells in the mammalian inner ear. *Proc. Natl. Acad. Sci. USA* **107**, 15798-15803.
Pan, B., Géléoc, G. S. G., Asai, Y., Horwitz, G. C., Kurima, K., Ishikawa, K., Kawashima, Y., Griffith, A. J. and Holt, J. R. (2013). TMC1 and TMC2 are components of the mechanotransduction channel in hair cells of the mammalian inner ear. *Neuron* **79**, 504-515.
Peng, Z., Wang, G.-P., Zeng, R., Guo, J.-Y., Chen, C.-F. and Gong, S.-S. (2013). Temporospatial expression and cellular localization of VGLUT3 in the rat cochlea. *Brain Res.* **1537**, 100-110.
Platzer, J., Engel, J., Schrott-Fischer, A., Stephan, K., Bova, S., Chen, H., Zheng, H. and Striessnig, J. (2000). Congenital deafness and sinoatrial node dysfunction in mice lacking class D L-type Ca2+ channels. *Cell* **102**, 89-97.
Raft, S. and Groves, A. K. (2015). Segregating neural and mechanosensory fates in the developing ear: patterning, signaling, and transcriptional control. *Cell Tissue Res.* **359**, 315-332.
Rauch, S. D., Velazquez-Villasenor, L., Dimitri, P. S. and Merchant, S. N. (2001). Decreasing hair cell counts in aging humans. *Ann. N. Y. Acad. Sci.* **942**, 220-227.
Rüsch, A., Lysakowski, A. and Eatock, R. A. (1998). Postnatal development of type I and type II hair cells in the mouse utricle: acquisition of voltage-gated conductances and differentiated morphology. *J. Neurosci.* **18**, 7487-7501.
Schmitz, F., Königstorfer, A. and Südhof, T. C. (2000). RIBEYE, a component of synaptic ribbons: a protein's journey through evolution provides insight into synaptic ribbon function. *Neuron* **28**, 857-872.
Seal, R. P., Akil, O., Yi, E., Weber, C. M., Grant, L., Yoo, J., Clause, A., Kandler, K., Noebels, J. L., Glowatzki, E. et al. (2008). Sensorineural deafness and seizures in mice lacking vesicular glutamate transporter 3. *Neuron* **57**, 263-275.
Sekerková, G., Zheng, L., Mugnaini, E. and Bartles, J. R. (2006). Differential expression of espin isoforms during epithelial morphogenesis, stereociliogenesis and postnatal maturation in the developing inner ear. *Dev. Biol.* **291**, 83-95.
Shen, Q., Wang, Y., Dimos, J. T., Fasano, C. A., Phoenix, T. N., Lemischka, I. R., Ivanova, N. B., Stifani, S., Morrisey, E. E. and Temple, S. (2006). The timing of cortical neurogenesis is encoded within lineages of individual progenitor cells. *Nat. Neurosci.* **9**, 743-751.
Shi, F., Cheng, Y.-F., Wang, X. L. and Edge, A. S. B. (2010). Beta-catenin up-regulates Atoh1 expression in neural progenitor cells by interaction with an Atoh1 3′ enhancer. *J. Biol. Chem.* **285**, 392-400.
Shi, F., Kempfle, J. S. and Edge, A. S. B. (2012). Wnt-responsive lgr5-expressing stem cells are hair cell progenitors in the cochlea. *J. Neurosci.* **32**, 9639-9648.

Development (2016) 143, 4381-4393 doi:10.1242/dev.139840

Shi, F., Hu, L. and Edge, A. S. B. (2013). Generation of hair cells in neonatal mice by beta-catenin overexpression in Lgr5-positive cochlear progenitors. *Proc. Natl. Acad. Sci. USA* **110**, 13851-13856.

Shi, F., Hu, L., Jacques, B. E., Mulvaney, J. F., Dabdoub, A. and Edge, A. S. B. (2014). beta-Catenin is required for hair-cell differentiation in the cochlea. *J. Neurosci.* **34**, 6470-6479.

Simmons, D. D., Tong, B., Schrader, A. D. and Hornak, A. J. (2010). Oncomodulin identifies different hair cell types in the mammalian inner ear. *J. Comp. Neurol.* **518**, 3785-3802.

Sommer, I. and Schachner, M. (1981). Monoclonal antibodies (O1 to O4) to oligodendrocyte cell surfaces: an immunocytological study in the central nervous system. *Dev. Biol.* **83**, 311-327.

Sommer, I. and Schachner, M. (1982). Cell that are O4 antigen-positive and O1 antigen-negative differentiate into O1 antigen-positive oligodendrocytes. *Neurosci. Lett.* **29**, 183-188.

Spoendlin, H. (1975). Retrograde degeneration of the cochlear nerve. *Acta Otolaryngol.* **79**, 266-275.

Toesca, A. (1996). Central and peripheral myelin in the rat cochlear and vestibular nerves. *Neurosci. Lett.* **221**, 21-24.

Tyler, W. A., Medalla, M., Guillamon-Vivancos, T., Luebke, J. I. and Haydar, T. F. (2015). Neural precursor lineages specify distinct neocortical pyramidal neuron types. *J. Neurosci.* **35**, 6142-6152.

Valderrama-Canales, F. J., Gil-Loyzaga, P. G., Merchan-Perez, A. and Lopez Sanchez, J. G. (1993). Astrocyte cytoarchitecture in cochlear nuclei of the rat: an immunocytochemical study. *ORL J. Otorhinolaryngol. Relat. Spec.* **55**, 313-316.

Wang, Y., Pang, Y.-W., Dong, Y.-L., Zhang, F.-X., Li, J.-L. and Li, Y.-Q. (2007). Localization of vesicular glutamate transporters in the peripheral vestibular system of rat. *Neurosci. Bull.* **23**, 175-179.

Witt, C. M., Hu, H. Y., Brownell, W. E. and Bertrand, D. (1994). Physiologically silent sodium channels in mammalian outer hair cells. *J. Neurophysiol.* **72**, 1037-1040.

Wong, A. C. Y. and Ryan, A. F. (2015). Mechanisms of sensorineural cell damage, death and survival in the cochlea. *Front. Aging Neurosci.* **7**, 58.

Wooltorton, J. R. A., Gaboyard, S., Hurley, K. M., Price, S. D., Garcia, J. L., Zhong, M., Lysakowski, A. and Eatock, R. A. (2007). Developmental changes in two voltage-dependent sodium currents in utricular hair cells. *J. Neurophysiol.* **97**, 1684-1704.

Yamamoto, N., Tanigaki, K., Tsuji, M., Yabe, D., Ito, J. and Honjo, T. (2006). Inhibition of Notch/RBP-J signaling induces hair cell formation in neonate mouse cochleas. *J. Mol. Med.* **84**, 37-45.

Yang, D., Thalmann, I., Thalmann, R. and Simmons, D. D. (2004). Expression of alpha and beta parvalbumin is differentially regulated in the rat organ of corti during development. *J. Neurobiol.* **58**, 479-492.

Yang, J., Bouvron, S., Lv, P., Chi, F. and Yamoah, E. N. (2012). Functional features of trans-differentiated hair cells mediated by Atoh1 reveals a primordial mechanism. *J. Neurosci.* **32**, 3712-3725.

Zhao, C., Deng, W. and Gage, F. H. (2008). Mechanisms and functional implications of adult neurogenesis. *Cell* **132**, 645-660.

Zheng, J., Shen, W., He, D. Z. Z., Long, K. B., Madison, L. D. and Dallos, P. (2000). Prestin is the motor protein of cochlear outer hair cells. *Nature* **405**, 149-155.